JOURNAL OF AIRCRAFT
Vol. 39, No. 1, January–February 2002

Low-Order Method for Predicting Aerodynamic Performance Degradation Due to Ground Icing

G. F. Syms*
National Research Council Canada, Ottawa, Ontario K1A0R6, Canada

A low-order method to compute the degradation in the maximum lift coefficient of an aircraft due to distributed surface roughness has been developed. The algorithm is applied to the Fokker F28 Mk1000, an aircraft involved in an accident in which ground icing was determined to play a significant role. The method consists of two complementary portions. The first uses a low-order panel method to compute the quasi-steady aerodynamic characteristics, in and out of ground effect, of the complete aircraft geometry including one- or two-element flaps, a boundary-layer fence, nacelles, and a horizontal tail. The numerical model then, in the second portion, generates an engineering estimate of the maximum lift coefficient for the aircraft configuration. The method is based on the assumptions that the pressure difference between the suction peak and the trailing edge of an airfoil is a maximum at the maximum lift coefficient and that the condition in which one spanwise station of a wing in a stripwise analysis violates this maximum pressure difference rule is the point at which the maximum lift of the entire aircraft is generated. The application of the pressure difference rule is modified to account for the presence of the boundary-layer fence and can estimate (on the conservative side) the effects of distributed surface roughness on the maximum lift coefficient using an appropriate maximum allowable pressure difference.

Introduction

TAKEOFFS and landings are integral parts of an aircraft's operation. They are, however, two of the most hazardous flight conditions because the aircraft is operating at high lift coefficients and angles of attack, on or near the ground. These maneuvers become potentially dangerous in adverse weather conditions such as snow and freezing precipitation often encountered in northern climates. An engineering method has been developed at the Aerodynamics Laboratory (AL) that can compute the effect of distributed surface roughness (ground icing) on the maximum lift coefficient of an aircraft.[1]

The aircraft analyzed in this paper is a Fokker F28 Mk1000, an aircraft that crashed outside of Dryden, Ontario, Canada in 1989. The investigation of the accident determined that wing contamination played a significant role in causing the crash.[2] The numerical model of the F28 has as its foundation a panel representation of the aircraft. The geometry includes part-span one- and two-element flaps, nacelles, a horizontal tail, and a boundary-layer fence.

Panel methods have been successfully applied to complete aircraft configurations.[3–7] Although a panel method by itself does not incorporate the effects of viscosity, methods are available that couple a panel code with either a two-dimensional[8] or three-dimensional boundary-layer calculation.[9] These algorithms will compute the loss of lift due to viscous effects, but they are limited by their inability to handle separated flows effectively. The current method takes into account the effects of viscosity by computing $C_{L_{\max}}$ via a stripwise analysis of the panel method results. The stripwise analysis is based on an algorithm proposed by Valarezo and Chin.[10]

The effect of surface roughness has been studied by other authors in two dimensions both experimentally[11,12] and computationally.[13,14] Progress is ongoing numerically in three dimensions, and these algorithms might eventually supplant the current one as they develop methods to handle separated flow regions.

The estimation of maximum lift coefficients of swept wings with flaps via a stripwise analysis has been studied experimentally.[15–17] In these studies, the two-dimensional criterion used to determine stall was the maximum lift coefficient of a section and not the maximum pressure difference, but the two are fundamentally the same.

In the following sections, the numerical model of the F28 is described including how the horizontal tail, ground effect, and boundary-layer fence are modeled. The method's ability to handle these complex phenomena increases the fidelity of the method beyond its initial form presented in Ref. 1. The model's lift curves are then compared to available data in and out of ground effect. The final set of results validate the model's ability to estimate the maximum lift coefficient for the F28 in and out of ground effect and with distributed surface roughness.

Method

The current numerical model estimates the maximum lift coefficient based on an algorithm proposed by Valarezo and Chin.[10] The method is based on the underlying postulate put forth by Smith,[18] which says that the maximum lift for a two-dimensional airfoil is generated when the difference in pressure between the suction peak and the trailing edge, ΔC_P, is at its maximum. The method is also based on the assumption that the condition in which one spanwise station of a wing in a stripwise analysis violates this maximum pressure difference rule is the point at which the maximum lift of the entire aircraft is generated.

The two components of the method are a three-dimensional flowfield and a maximum pressure difference criterion. The flowfield can be computed from any computationally efficient inviscid solver (panel or Euler) because the viscous effects are considered in the application of the maximum pressure difference rule. The method implemented at the AL uses the three-dimensional panel method PMARC.[19] In the original Valarezo and Chin method,[10] the authors summarized a large set of experimental data to generate an generic set of pressure difference curves that show both Mach number and Reynolds number dependence (Fig. 1). The current implementation of the method use a two-dimensional panel method with a coupled boundary-layer code to predict the maximum pressure difference allowed for a particular airfoil section. The use of this code allows the effect of surface contamination on the maximum lift coefficient to be taken into account.

Presented as Paper 2001-1005 at the AIAA 39th Aerospace Sciences Meeting and Exhibit, Reno, NV, 8–11 January 2001; received 12 May 2001; revision received 23 October 2001; accepted for publication 24 October 2001.

*Research Officer, Aerodynamics Laboratory, Institute for Aerospace Research.

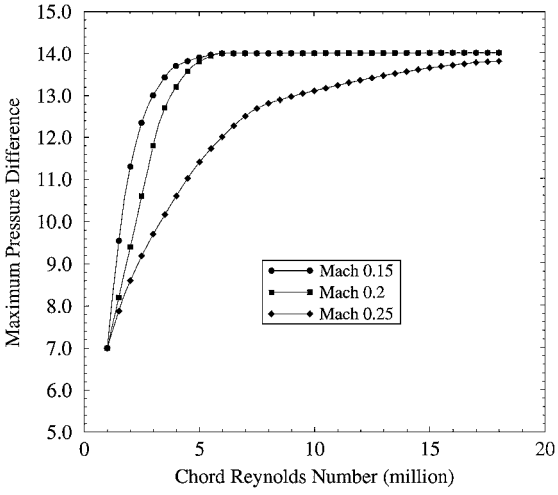

Fig. 1 Pressure difference rule criteria from Ref. 10.

The effect of distributed surface roughness on the maximum lift coefficient of a particular geometry can be determined by using a set of pressure difference curves that incorporate the effect of roughness on two-dimensional wing sections. When the same method is applied to both clean and roughened airfoils, it is assumed that the stalling mechanism for the wing is the same for the two cases. That is, if the wing experiences a trailing-edge stall without surface contamination, then the roughened wing also undergoes a trailing-edge stall. Surface roughness can have a drastic impact on the stalling characteristics of a wing, to the point that the preceding assumption is erroneous. Although the physical stall is a three-dimensional phenomenon, the two-dimensional analysis to determine the maximum pressure difference allowed at a wing section could indicate a change in the stall behavior. In the situation where a change occurred, it would be inappropriate to apply the method described here.

The pressure difference rule is a stripwise analysis of an inviscid flowfield to determine an estimate of the maximum lift coefficient of the entire wing. It assumes that all of the viscous effects are generally locally two dimensional in nature. Thus, any object or wing feature (such as a kink in the wing or a boundary-layer fence) that creates a three-dimensional boundary-layer phenomenon will decrease the accuracy of the computed estimate of $C_{L_{\max}}$. Modifications to the pressure difference rule criterion that account for the presence of the boundary-layer fence are discussed later.

The method used to generate the maximum pressure difference criterion for the F28 wing sections must be efficient and capable of determining the effects of roughness on the aerodynamic performance of the section. A lift curve must be generated for each roughness condition for each wing section to determine the pressure difference at $C_{l_{\max}}$. Also, the maximum ΔC_P must be determined for both flapped and unflapped airfoil sections. To this end, a two-dimensional panel method coupled with a boundary-layer calculation generated the required criteria. The code used is a combination of a low-order panel method coupled with a boundary-layer calculation.[14] The effect of surface roughness was included by using the method of Dvorak.[20] In that method, Dvorak modifies the law of the wall to create an equation that relates to the skin-friction coefficient to the boundary-layer momentum thickness, the inviscid surface flow speed, the roughness height k, and the dimensionless roughness spacing λ. Boundary-layer corrections were made for both the main element and the flap, in the two-element version of the code. These calculations are adequate for the 18-deg single-element flap geometry, but the F28 wing's flap consists of a vane and a flap when deployed at 30 and 42 deg. Because pressure differences for these specific airfoils could not be generated with the tools at hand, it is assumed that the maximum ΔC_P computed for the 18-deg single-element flap geometry holds for the higher flap angles.

The geometry for the F28 Mk1000 was obtained from Fokker Aircraft B.V. The aircraft geometry includes wings, one- and two-element flaps, a fuselage, nacelles, a boundary-layer fence, and the horizontal stabilizer. Not included are the vertical tail and the landing gear. The engine intake and exhaust are not modeled because their effect on the wings was assumed to be negligible. (The engines are rear-fuselage mounted.) It is also known that the rear-mounted engines of the F-28 do not significantly affect the lift of the aircraft but rather its pitching moment. Thus, nacelles are hollow allowing air to flow through.

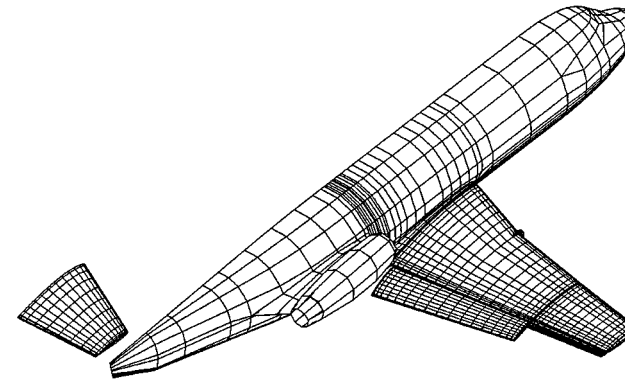

Fig. 2 F28 paneling with 18-deg flap.

For the symmetric flight conditions considered in this paper, half of the aircraft was paneled (Fig. 2). There are approximately 2000 panels on the wing and flap, 300 panels on the tail, and 700 panels on the fuselage and nacelles.

The horizontal tail was not included in the geometry supplied by Fokker Aircraft. However, the contribution of the tail to the lift of the whole aircraft can be deduced from experimental data. Reference 21 contains information on the pitching moment of the aircraft with and without the horizontal tail. The difference between the two sets of values is the contribution to pitching moment of the tail's lift. Although the geometry of the horizontal tail is known, the airfoil section of the stabilizer is not. Through a little trial and error with several NACA airfoil sections, a section was selected that provided a reasonable representation of the lifting characteristics of the tail.

Ground effect is incorporated into a takeoff simulation through the use of the method of images. The entire panelled geometry (aircraft and wake) is mirrored in the ground plane with the opposite sign for the source and doublet distributions. This means, at the ground plane, there is no normal velocity, only a tangential component. This is equivalent to a slip boundary condition because no boundary layer is allowed to grow on the ground plane.

The F28 Mk1000 includes a boundary-layer fence (Fig. 2). The fence extends 15% chord aft of the leading edge (on the upper and lower surfaces of the wing) and is 3.3% chord high. It is located at 33% semispan on the full-scale aircraft and on the wind-tunnel model used for roughness tests, and at 41% semispan on the smooth-surface tunnel model. The change in location from the original model to the aircraft was due to analyses performed during flight tests.[22] The purpose of the fence is to restart the boundary layer on the wing. The effect it has on the stall of the wing is twofold: 1) It promotes inboard stall; 2) It delays outboard stall.[22] Locally, the fence will generate a vortex behind it that will scour the nearby surface of the wing. The fence is included in the paneling of the aircraft as a Neumann sheet, which means the normal velocity to the fence is continuous across the sheet. This is the same as treating the fence as an infinitely thin wing. To be consistent in treating the fence as a wing, a vortex sheet should be shed off the trailing edge of the fence, but this sheet is not modeled in this work. It is believed that only small errors in the pressure distribution on the wing are incurred by omitting it even at fairly large aircraft yaw angles (which is equivalent to large angles of attack for the fence).

Because the effects of the boundary-layer fence on the wing are primarily viscous in nature, the main treatment of the fence is in the application of the maximum pressure difference criterion. To model the proper stalling of the wing, the criterion is modified by reducing the maximum allowable pressure difference at the fence (by a suitable factor) and by smoothing the jump in the criterion

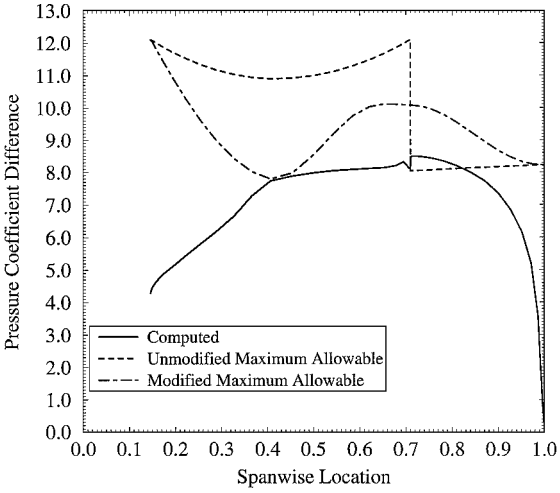

Fig. 3 Modification of pressure difference rule for modeling of boundary-layer fence.

at the flap-edge wing station (Fig. 3). This smoothing is necessary outside considerations of the fence because at that particular spanwise location, when strictly applying the criterion, there are two different maximum pressures allowed, depending on from which direction that wing section is approached (flapped vs unflapped). It is assumed that the same fence $\Delta C_{P_{\max}}$ reduction factor and smoothing hold for clean and rough wings. Because the application of the maximum pressure difference rule accounts for the effects of viscosity in the flow, it is assumed that the factor required to modify the rule to account for the different stalling behavior of the wing is Reynolds number dependent. This means that there will be different values of the factor at model scale and at flight Reynolds numbers.

Results and Discussions

Lift Curves

Out of Ground Effect

The first step in computing the maximum lift of the aircraft is to compute the lift curves for the given geometry using the three-dimensional panel method. To this end, the lift curves have be computed for the F28 for several flap deflections and at two different scales.

The F28 Mk1000 in free air was simulated with flap deflections of 18 deg (typical for takeoff) and 30, and 42 deg (both typical for landing). Experimental data were available at both model scale (1:20) and full scale (1:1). At model scale, the freestream conditions were $M_\infty = 0.19$ with a Reynolds number (based on mean aerodynamic chord) of 2.7×10^6. The flight conditions were for $M_\infty = 0.16$–0.21 with a corresponding Reynolds number of 11–14×10^6. The calculations were done with a freestream velocity of 64 m/s at full scale and 56 m/s at model scale. The Prandtl–Glauert correction was applied to account for compressibility effects. The tail was kept at a constant deflection to mimic the experiments (both model and full scale). Figures 4 and 5 show the comparisons of the simulations to the measured data. The panel method calculations were carried out up to and beyond the expected stall. A later stage of the analysis will indicate where on the curves one should stop to get an approximation of $C_{L_{\max}}$. Figures 4 and 5 show that as expected the panel method overpredicts both the lift and the slope of the curve. This overprediction is because panel methods lack the effects of viscosity, the effects being greater at higher flap angles (and consequently high lift coefficients).

One method to correct for the inadequacies of the potential method is to reduce the flap angle. This will account for the decambering effect of the boundary layers and wakes on multielement wings.[10] In the current study, the flap for the 18-deg case is reduced to 16.4 deg, so that the computed curve matches the experimental data in the region of interest (high C_L). Matching the lift curves means that the pressure difference method will generate a reasonable approximation to the pitch angle at maximum lift, as well as the maximum lift coefficient itself. Although possible, the flap was not modified for the 30- and 42-deg cases. It was unclear as to what the necessary flap motion would be because at the higher deflections, the flap splits into two elements. This, however, should not affect the calculation of maximum lift because it is based on a pressure difference independent of how it is produced.

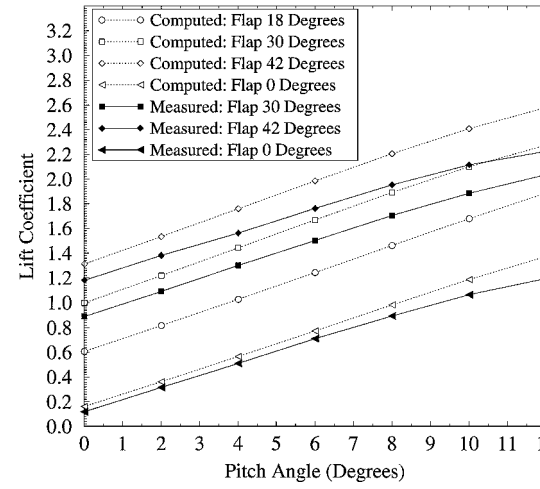

Fig. 4 Lift coefficient: model scale, out of ground effect.

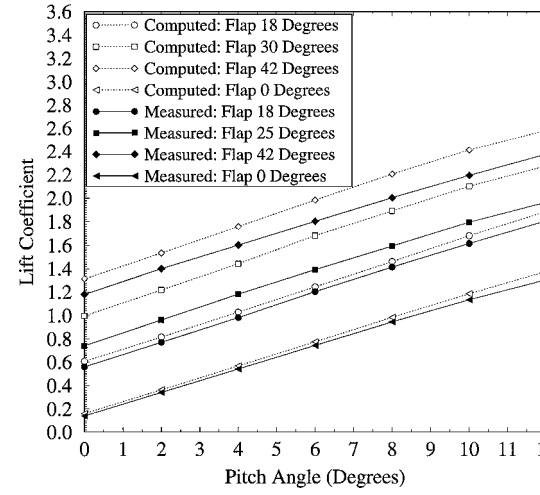

Fig. 5 Lift coefficient: full scale, out of ground effect.

In Ground Effect

The effect of the ground plane on the aircraft is a complex and not well-understood phenomena. Lift coefficients and lift curve slopes can vary significantly depending on the simulation undertaken. Flight tests show an increase in lift and lift curve slope for all flap angles for very low heights above the ground.[21,23] Wind-tunnel experiments show a smaller increase in slope accompanied by a shift to higher lift coefficients.[21] Theoretical analyses, based on potential theory arguments, show a decrease in lift curve slope with an increase in lift at low C_L and a decrease in lift at high C_L (Ref. 24).

The current analysis uses the method of images to simulate the ground plane. Two sets of results are computed, one at model scale and one at full scale. For conciseness, only the second set of results are presented here. For the full-scale simulations at the four flap angles (0, 18, 30, and 42 deg), the wheels are in contact with the ground, and the point of rotation is taken to be that point of contact. This puts the center of gravity 2.46 m off the ground at 0-deg angle of attack ($h_{\mathrm{MAC}}/c = 0.7$). The tail is set at a constant deflection for all of these cases. Figure 6 shows the lift curves for these simulations and the equivalent full-scale measurements. It can be seen that the panel method underpredicts the effect of the ground on the aircraft.

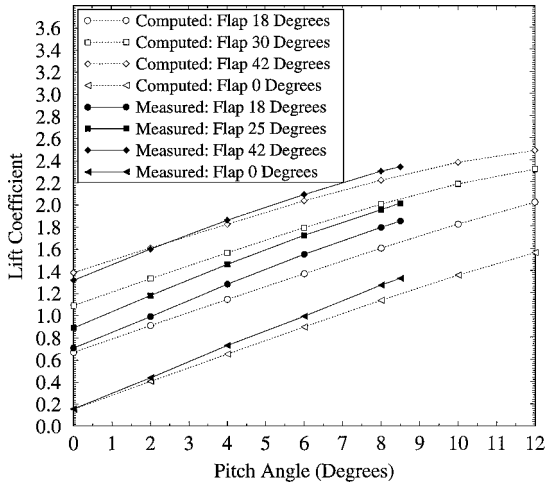

Fig. 6 Lift coefficient: full scale, in ground effect, wheels in contact with ground.

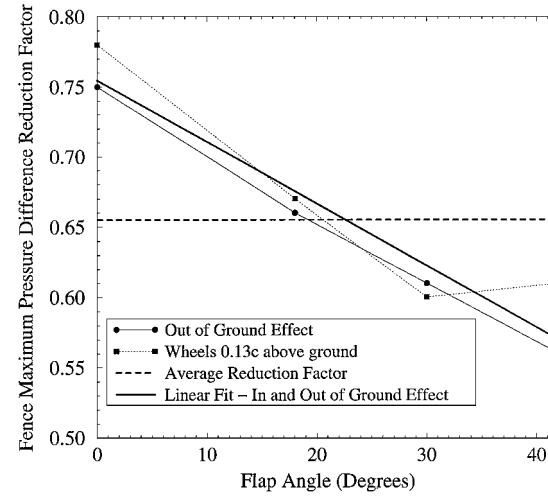

Fig. 7 Fence maximum ΔC_p reduction factor: model scale.

The flap angle can be modified to attempt to compensate for the observed discrepancies between computed and full-scale lift coefficients. This will be slightly more difficult than the free-air flap modification because of the larger difference in lift curve slopes in ground effect. However, if the flap angle is increased to 26.8 deg, then a fairly good match can be achieved at the high angles of attack in ground effect. A linear transition from the in ground effect flap geometry to free-air geometry blends the two modifications as a function of height of center of gravity above the ground. It is assumed that the ground effect decreases to a negligible amount when the wing is one span above the ground.[23]

Maximum Lift Coefficient

Clean Wing Surface

In the current analyses, the first step in the estimation of the maximum lift coefficient of an aircraft geometry is the calculation of the lift curve. The second step is the application of the maximum pressure difference rule to determine where on the curve the $\Delta C_{P_{\max}}$ criterion is violated, indicating that the maximum lift has been reached. Note that the pressure difference rule can be applied to any particular flight attitude yielding a true or false answer as to whether the aircraft is flying at a condition beyond maximum lift. The criterion is applied to a sequence of increasing angles of attack providing an estimate of $C_{L_{\max}}$.

In the algorithm of applying the pressure difference rule, first the $\Delta C_{P_{\max}}$ reduction factor of the fence must be determined. That is, the algorithm must be tuned to have the proper stall behavior. This would be true of any wing feature that would cause severe three dimensionality of the wing's boundary layer. To ascertain the appropriate reduction factor, a series of tests was performed in which the factor required to return the measured maximum lift (as reported in Ref. 21) was computed by trial and error. Figure 7 shows the results of these tests at model scale. It can be seen that a linear fit to the data would provide a reasonable approximation to the required fence factor both in and out of ground effect. Thus, only one value need be used for any particular flap setting. Figure 8 shows the results of using both a constant fence factor as well as a linearly varying reduction factor in the calculation of the maximum lift coefficient in free air. The agreement between the measured and computed maximum lift coefficients is quite good with a very positive comparison being seen at 18-deg flap deflection.

The determination of the appropriate fence reduction factor is more difficult at flight Reynolds numbers due to the scarcity of reliable data at or near stall, especially in ground effect. The maximum lift coefficient reported in Ref. 21 for the aircraft out of ground effect differs from that given in Ref. 23 for in ground effect because the first is based on lift and the second is based weight of the aircraft. In particular, the free-air $C_{L_{\max}}$ is given as an Federal Aviation Administration stall value defined as $\mathrm{d}V/\mathrm{d}t = 1$ kt/s. Because of the

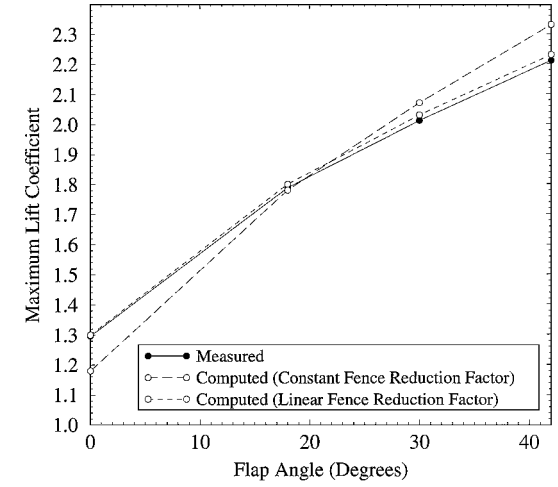

Fig. 8 Maximum lift coefficient: model scale, free air.

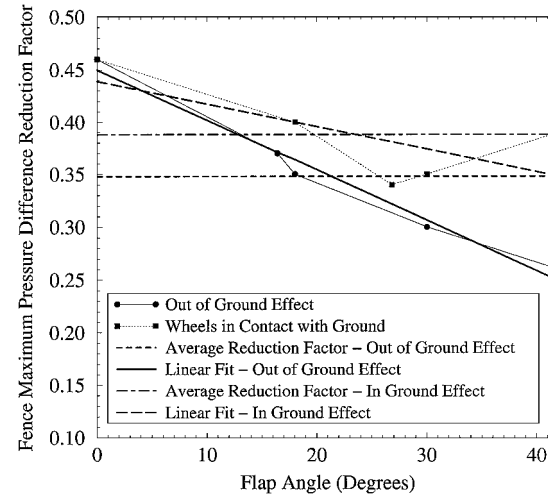

Fig. 9 Fence maximum ΔC_p reduction factor: full scale.

disparate sources of information, two sets of fence reduction factors had to be determined. They are given in Fig. 9. A linear fit is determined for conditions in ground effect and one for out of it. Applying the modified pressure difference rule out of ground effect yields the estimates of $C_{L_{\max}}$ seen in Fig. 10. Included is an estimate of the maximum lift with the modified flap angle of 16.4 deg. Calculations with the modified flap angle, which generate a better match to the measured lift curves compared to that generated using the geometric

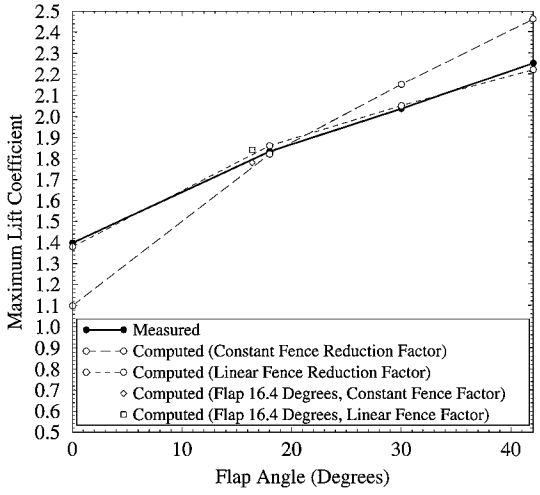

Fig. 10 Maximum lift coefficient: full scale, free air.

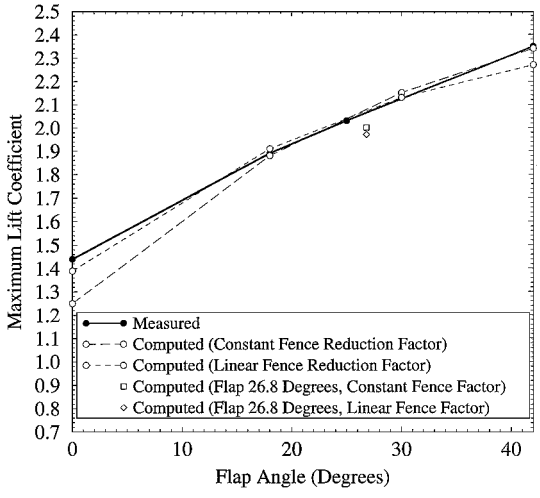

Fig. 11 Maximum lift coefficient: full scale, in ground effect, wheels in contact with ground.

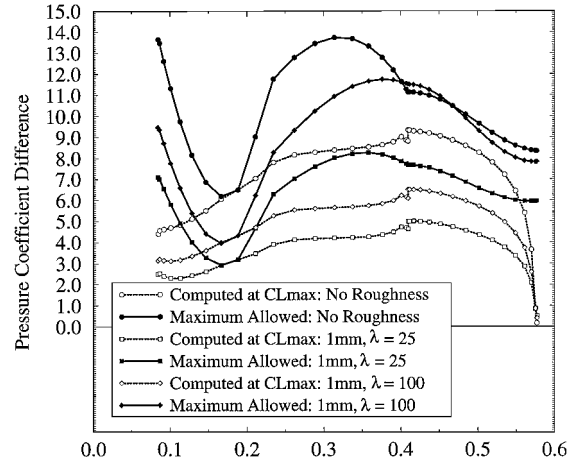

Fig. 12 Maximum pressure difference: model scale, various roughness conditions.

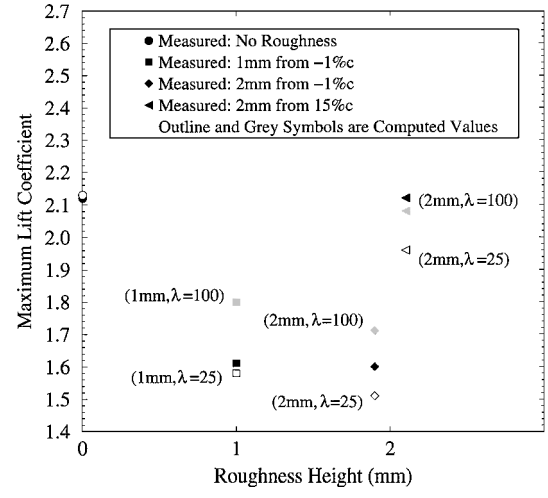

Fig. 13 Maximum lift coefficient: model scale, various roughness conditions.

18-deg flap, produce a slightly more accurate estimate of the maximum lift coefficient relative to the estimate using the 18-deg flap deployment.

Applying the second set of fence reduction factors to the set of lift curves in ground effect gives the estimates of maximum lift found in Fig. 11, showing reasonable agreement between measured and computed values. Included in Fig. 11 is the estimate of $C_{L_{\max}}$ with the flap at 26.8 deg, which was increased to match the computed lift curve with the measured one. This $C_{L_{\max}}$ estimate is fairly high, whereas the estimate generated using the geometric flap angle estimate is fairly accurate.

Distributed Surface Roughness

The final test of the algorithm is the application of the pressure difference rule to estimate the maximum lift coefficient for wings covered with distributed surface roughness. The amount of data published that documents the effects of roughness on complete aircraft configurations is extremely limited. What is available for the F28 is a set of runs performed at model scale with the flaps deployed to 30 deg (Ref. 23).

Before the criterion can be applied, the maximum pressure difference allowed accounting for the effects of roughness must be computed. To be able to do this, the roughness must be characterized in terms of a roughness height to chord ratio k/c and a roughness spacing λ. The characterization of physical roughness by these two numbers is an approximation that condenses a large body of physics into two global parameters. Two different types of roughnesses were used in the experiment: 1- and 2-mm full-scale distributed to a density of approximately 1/cm^2. The roughness covered the upper surface of the airfoil and continued around the leading edge to 1% chord aft of the leading edge on the undersurface of the wing. A third roughness case measured had the 2-mm roughness beginning at 15%c of the upper surface. For a mean aerodynamic chord of 3.505 m, the resulting k/c values are 0.000285 and 0.000571. To estimate the spacing parameter λ, the formula

$$\lambda = D^2/A_f \tag{1}$$

where A_f is the frontal area of the roughness element and $1/D^2$ is the number of significant roughness elements per unit surface area, is used.[25] If a square cross section is assumed for a roughness element, then A_f has the values 1×10^{-6}m^2 and 4×10^{-6}m^2 for the 1- and 2-mm heights, respectively. For a 1/cm^2 distribution, the estimates of λ become 100 and 25 for the two roughness heights. The numbers can be thought of as most likely on the low side because the assumption of a square frontal cross section most likely provides a larger number than present in the experiment.

Thus, when the roughness is characterized, a new set of pressure difference curves required for the wing can be computed (Fig. 12). To estimate the sensitivity of $C_{L_{\max}}$ to λ, both spacing estimates were used for each roughness height. The experimental data for the aircraft with roughness were reported at model scale with the fence at wing station 3784. This means that the $\Delta C_{P_{\max}}$ reduction factor computed in the preceding section with the fence at location 4700 cannot be used. The required fence factor is determined by matching the maximum lift coefficients for the clean configuration ensuring the

correct stalling behavior for the wing. This factor is then applied to the roughened wing cases. Figure 13 shows the estimates of the maximum lift coefficient under the various roughness conditions for the 30-deg flap configuration. The computed $C_{L_{max}}$ bound the measured values for the cases with roughness starting on the undersurface of the wing, but overestimates the loss of maximum lift for the roughness distribution starting on the upper surface. For this last case, the roughness begins past the suction peak on the upper surface of the wing section, and thus, its effect on the section's performance is not as great as that with the roughness starting near the stagnation point.

Summary

An engineering analysis has been developed to estimate the maximum lift coefficient of a complete aircraft geometry. The method is based on a two-dimensional stripwise analysis of a three-dimensional pressure field. Its foundation is the assumptions that the maximum difference in pressure between the suction peak and the trailing edge of an airfoil occurs at maximum lift and that $C_{L_{max}}$ is reached when any one spanwise station on a wing violates this criterion. It is also assumed that this criterion holds for both clean and roughened wings.

The three stages of the algorithm (aircraft surface pressure calculation, maximum allowed pressure difference determination, and application of pressure difference rule) have their own limitations. The calculation of the pressure distribution on the wing is governed by the limitations of the three-dimensional panel method. The three-dimensional calculation is a quasi-steady analysis that excludes viscous effects. This means that for any given configuration the lift will be overpredicted. Geometry adjustments, such as flap angle modification, can be made to account for this in part.

The calculation of the maximum pressure difference allowed is done using a two-dimensional panel method coupled with a boundary-layer calculation. This code will produce estimates of the performance of one- and two-element airfoils. The accuracy of the pressure difference criterion relies on the fidelity of these simulations.

Finally, the application of the pressure difference rule had to be modified to take into account the boundary-layer fence. This wing feature is designed to affect the boundary-layer and stalling characteristics of the wing. A factor reducing the maximum pressure allowed on the wing sections near the fence moved the critical section of the wing from near the outer edge of the flap to the fence location. The factor's value is Reynolds number and flap-angle dependent.

The presented algorithm has shown the ability to compute an accurate estimate of the maximum lift coefficient both in and out of ground effect. The method also can predict the degradation due to surface roughness, but is conservative in its estimates. One challenge in being able to simulate the effects of ground icing is the characterization of the ice. The algorithm must to be tuned to produce the proper stalling behavior and, thus, depends on the accuracy and availability of data used in the tuning. If a reasonable representation of the lift curve and stall angle is developed, as has been done for the 18-deg flap geometry, then the pressure difference rule can be applied to any flight attitude to determine if the aircraft is in a poststall condition. Further extensions to the algorithm would have to be made if any information is to be extracted from the lift coefficients of all or part of a stalled or partially stalled wing. The method is computationally efficient and provides a useful engineering tool, but could eventually be replaced by three-dimensional methods applicable to separated flows.

Acknowledgments

This work was funded in part by Transport Canada Aviation. The geometry for the F28 was supplied by Fokker B.V., and the help of Dr. Jack vanHengst, then of Fokker, especially concerning the aerodynamics of the F28 is greatly appreciated. Initial implementation of the pressure difference rule was done by Mattijs Janssens.

References

[1] Syms, G. F., Crabbe, R. S., and Janssens, M., "The Prediction of the Effect of Icing on Wing Maximum Lift," *Proceedings of the Fifth Aerodynamics Symposium of the Canadian Aeronautics and Space Inst.*, Montreal, May 1995.

[2] Moshansky, V. P., "Commission of Inquiry into the Air Ontario Crash at Dryden, Ontario—Final Report," Minister of Supply and Services, Canada, 1992.

[3] Edge, D. C., and Perkins, J. N., "Three-Dimensional Aerodynamic Analysis of a Subsonic High-Lift Transport Configuration Using PMARC," AIAA Paper 95-0039, 1995, pp. 561–570.

[4] Roggero, F., and Larguier, R., "Aerodynamic Calculation of Complex Three-Dimensional Configurations," *Journal of Aircraft*, Vol. 30, No. 5, 1993.

[5] Joosen, C. J. J., and Sytsma, H. A., "Application of the NLR Panel Method to a Swept-Wing/Body Combination with Part-Span Flaps at Low Speed and Comparison with Experimental Results," National Aerospace Laboratory, Amsterdam, The Netherlands, NLR TR 80030 U, 1982.

[6] Donham, R. E., Dupcak, J. D., and Conner, F., "Application of A Panel Method (QUADPAN) to the Prediction of Propeller Blade Loads," Society of Automotive Engineers, SAE Rept. 861743, 1986.

[7] Tinoco, E. N., and Rubbert, P. E., "Panel Methods—PAN AIR," *Computational Methods in Potential Aerodynamics*, Computational Mechanics/Springer-Verlag, Berlin, 1985, pp. 40–91.

[8] Maskew, B., "Program VSAERO Theory Document: A Computer Program for Calculating Non-Linear Aerodynamic Characteristics of Arbitrary Configurations," NASA CR 4023, 1987.

[9] Crabbe, R. S., "Simple Numerical Method to Compute Viscous Lift Loss of Wings," *Journal of Aircraft*, Vol. 35, No. 1, 1998, pp. 27–32.

[10] Valarezo, W. O., and Chin, V. D., "Method for the Prediction of Wing Maximum Lift," *Journal of Aircraft*, Vol. 31, No. 1, 1994, pp. 103–109.

[11] Valarezo, W. O., "Maximum Lift Degradation Due to Wing Upper Surface Contamination," *Proceedings of the 1st Bombardier International Workshop*, Aircraft Icing/Boundary-Layer Stability and Transition, Montreal, Canada, Sept. 1993.

[12] Boer, J. N., and van Hengst, J., "Aerodynamic Degradation due to Distributed Roughness on High Lift Configuration," AIAA Paper 93-0028, 1993, pp. 104–112.

[13] Kind, R. J., and Lawrysyn, M. A., "Performance Degradation Due to Hoar Frost on Lifting Surfaces," *Canadian Aeronautics and Space Journal*, Vol. 38, No. 2, 1992, pp. 62–70.

[14] Crabbe, R. S., "Predicted Influence of Fluid Runback Waves on Airfoil Lift," *Proceedings of the 4th Annual Conference of the CFD Society of Canada*, Ottawa, June 1996, pp. 123–126.

[15] Pearson, H. A., and Anderson, R. F., "Calculation of the Aerodynamic Characteristics of Tapered Wings with Partial-Span Flaps," NACA Rept. 665, 1939.

[16] Anderson, R. F., "Determination of the Characteristics of Tapered Wings," NACA Rept. 572, 1940.

[17] Maki, R. L., "The Use of Two-Dimensional Section Data to Estimate the Low-Speed Wing Lift Coefficient at Which Section Stall First Appears on a Swept Wing," NACA RM A51E15, 1951.

[18] Smith, A. M. O., "High-Lift Aerodynamics," AIAA Paper 74-939, 1974.

[19] PMARC Theory Manual and User's Guide, COSMIC Program No. ARC-12642, University of Georgia Research Foundation.

[20] Dvorak, F. A., "Calculation of Turbulent Boundary Layers on Rough Surfaces in Pressure Gradient," *AIAA Journal*, Vol. 7, No. 9, 1969, pp. 1752–1759.

[21] van Doorn, J. T. M., Erkelens, L. J. J., Han, S. O. T. H., and Kho, Y. G., "Comparison of Fokker F28 Wind Tunnel and Flight Data—A Summary," National Research Laboratory, Amsterdam, The Netherlands, NLR Rept. TR 73007 U, 1974.

[22] Schuringa, T., "Aerodynamics of Wing Stall of the Fokker F28," CP-102, AGARD, Paper 20, 1972.

[23] Morgan, J. M., Wagner, G. A., and Wickens, R. H., "A Report on the Flight Dynamics of the Fokker F28 Mk1000 as they Pertain to the Accident at Dryden, Ontario, March 1989," Commission of Inquiry into the Air Ontario Crash at Dryden, Ontario—Final Report, Technical Appendix 4, Ottawa, 1992.

[24] Torenbeek, E., *Synthesis of Subsonic Airplane Design*, Delft Univ. Press, Delft, The Netherlands, 1976.

[25] Simpson, R. L., "A Generalized Correlation of Roughness Density Effects on the Turbulent Boundary Layer," *AIAA Journal*, Vol. 11, 1973, pp. 242–244.